Supporting Information for

A naphthalimide-based fluorescent probe for highly selective detection of histidine in aqueous solution and its application in *in-vivo* imaging

Hio-Ieng Un,‡[a] Shuai Wu,‡[b] Chang-Bo Huang,[a] Zheng Xu[c] and Lin Xu*[a]

[a]*Shanghai Key Laboratory of Green Chemistry and Chemical Processes, Department of Chemistry, East China Normal University, 3663 N. Zhongshan Road, Shanghai 200062, China, E-mail: lxu@chem.ecnu.edu.cn*

[b]*Neurology Department of Changhai Hospital, The Second Military Medical University, Shanghai 200433, P. R. China.*

[c]*Chongqing Key Laboratory of Environmental Materials and Remediation Technology, College of Materials and Chemical Engineering, Chongqing University of Arts and Sciences, Chongqing 402160, China.*

Contents:

1. General information
2. Synthesis of probe **NPO** and model compounds **NPA** and **M1**–**3**
3. The absorption and emissive properties of **NPO** on changing the pH
4. The absorption and emissive properties of **NPC** on changing the pH
5. Fluorescence emission response of **NPO** in the presence of various metal ions
6. Fluorescence titration of **NPO** with Cu^{2+}
7. UV-Vis absorption titration spectra of **NPO** with Cu^{2+}
8. Fluorescence and absorption spectra of **NPC** in the presence of various amino acids
9. UV-Vis absorption titration spectra of **NPC** with His
10. The Job's plots of **NPO** with Cu^{2+} and **NPC** with His
11. Fluorescence emission response of **NPA**-Cu^{2+} and **M1**-Cu^{2+} in the presence of various metal ions
12. The cytotoxicity of probe **NPO** against HeLa cells

1. General information

Unless otherwise mentioned, all the reagents were of analytic grade. ^{1}H NMR and ^{13}C NMR spectra were measured on a Bruker AM-400 spectrometer with chemical shifts reported as ppm (in $CDCl_3$). Mass spectrometry data were obtained with a HP 5989A spectrometer. Absorption spectra were determined on a Varian Cary 100 Spectrophotometer. Fluorescence spectra were determined on a Varian Cary Eclipse.

The metal salts used were $Fe(ClO_4)_2$, $Zn(ClO_4)_2 \cdot 6H_2O$, $Co(ClO_4)_2 \cdot 6H_2O$, $Ni(ClO_4)_2 \cdot 6H_2O$, $Ba(ClO_4)_2 \cdot 3H_2O$, $Pb(ClO_4)_2 \cdot 3H_2O$, $Cd(ClO_4)_2 \cdot 6H_2O$, $Cu(ClO_4)_2 \cdot 6H_2O$, $Mn(ClO_4)_2 \cdot 6H_2O$, $LiClO_4 \cdot 3H_2O$, $NaClO_4 \cdot H_2O$, $AgClO_4 \cdot H_2O$, $Hg(ClO_4)_2 \cdot 3H_2O$, $Mg(ClO_4)_2 \cdot 6H_2O$, $Al(ClO_4)_3 \cdot 9H_2O$.

Hela cells were obtained from Institute of Basic Medical Sciences (IBMS) of Chinese Academy of Medical Sciences (CAMS), and grown in DMEM (High glucose) medium supplemented with 10% FBS. Cells were incubated in a 5% CO_2 humidified incubator at 37 ^{o}C and typically passaged with sub-cultivation ratio of 1:3 every two days.

Growing Hela Cells in the exponential phase of growth on 35-mm glass-bottom culture dishes (Φ 20mm) for 1-2 days to reach 70-90% confluency. These cells were used in fluorescence imaging experimentation. The cells were washed with DMEM for three times, and then incubated with 2 mL DMEM containing probe (10 μM) and in an atmosphere of 5% CO_2 and 95% air for 30 min at 37 °C. Cells were washed twice with 1 mL PBS at room temperature, and then followed by addition of 1 mL PBS and observed under Leica TCS SP5 II confocal laser scanning microscopy using HC × PLAPO 63X oil objective (NA, 1.40), with excitation by 405 nm and 500-700 nm emission light was collected. For the Cu^{2+} treated samples, cells were pre-washed twice, and incubated with 10 μM probe in DMEM for 30 minutes at 37 ^{o}C. After the removal of extracellular free probes by washing for three times, the cells were then incubated with 20 μM Cu^{2+} for 30 minutes at 37 ^{o}C. Cells were washed twice before observation under confocal microscopy in PBS. For the histidine treated samples, cells were pre-washed twice, and incubated with 10 μM probe in DMEM for 30 minutes at 37 ^{o}C. After the removal of extracellular free probes by washing for three times, the cells were then incubated with 20 μM Cu^{2+} for 30 minutes at 37 ^{o}C. Cells were washed twice with PBS, and then 250 μM histidine was added and incubated for further 30 minutes. Cells were washed with PBS for three times before observation under confocal microscopy in DMEM.

The larval stage 4 (L4) *C.* elegans was used. The L4 stage nematodes were washed three times with PBS. To expose the L4 stage nematodes to probe, a centrifuge tube was first filled with 1 mL of PBS buffer solution supplemented with 10 μM of probe **NPO**. These L4 stage worms were then incubated in the tubes at room temperature for 2.5 h. After the incubation, the exposed nematodes were washed three times again with PBS. Then the L4 stage nematodes were exposed at the Cu^{2+} aqueous solution, a centrifuge tube was filled with 1 mL of PBS buffer solution supplemented with 20 μM of Cu^{2+} which was incubated at room temperature for 3 h. For the histidine treated samples, the previously exposed worms were incubated in centrifuge tube filled with 1 mL of PBS buffer solution, containing 250 μM of histidine, at 25 °C for 3 h. The nematodes were washed three times again with PBS before being mounted onto a slide glass. Fluorescence imaging of the mounted nematodes were performed with Olympus BX51 fluorescence microscope U-FGW Ex 530−550 (Em 575 nm) channel.

The cytotoxicity of a probe **NPO** against HeLa cells was measured by using the standard methyl thiazolyl tetrazolium (MTT) assay. The cells were seeded into 96-well cell culture plate at 5×10^3/well in complete medium (DMEM containing 10% fetal bovine serum (FBS)). Cells were incubated for 24 h at 37 ^oC under 5% CO_2 to allow attachment of the cells. After removal of the medium and washing with PBS for three times, cells were incubated with fresh medium containing various concentrations of probe for 24 h, at 37 ^oC under 5% CO_2. Next, 80 mL fresh DMEM was added to replace the medium with different concentrations of probe, which was followed by addition of another 20 mL fresh DMEM containing 5 $mg\cdot mL^{-1}$ of MTT. After the cells were allowed to incubate with MTT for 4 h, the supernatant was removed and 150 mL DMSO was loaded into each well to dissolve the formazan under shaking for 10 min. Then the cell viability was determined by measuring the light absorbance at 570 nm with a microplate reader. Each data point was collected by averaging the values of three wells, and untreated cells were used as controls. Percentage cell viability was calculated by comparing the absorbance of the control cells to that of treated cells.

2. Synthesis of probe NPO and model compounds NPA and M1–3

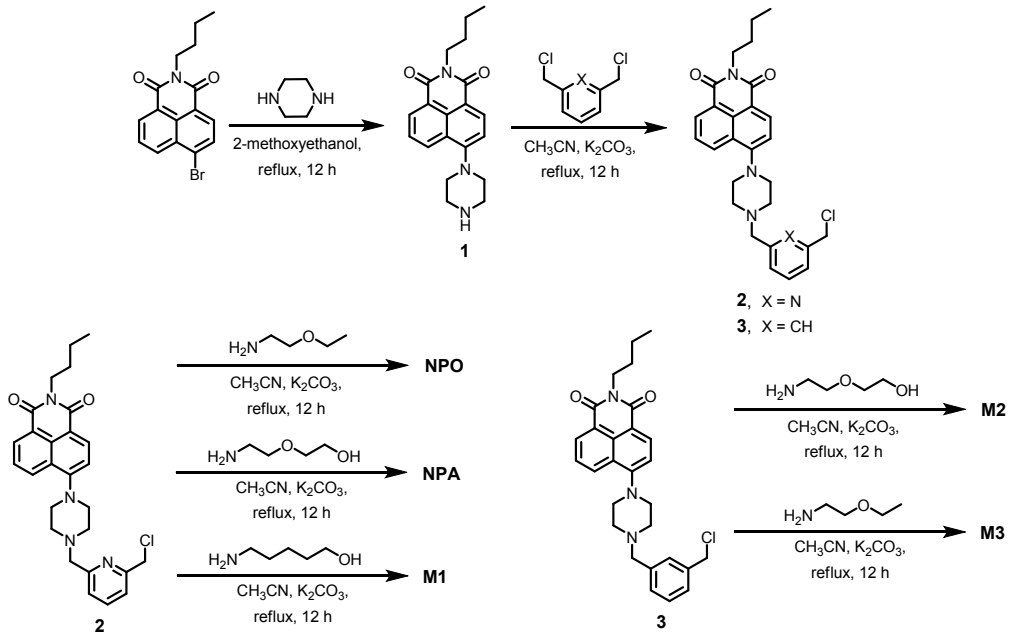

The compounds **NPO**, **NPA**, **M1**, and **M2** were prepared according to our previous report (*Chem. Asian J.*, 2014, **9**, 3397).

Compound **M3**: Anhydrous potassium carbonate (138 mg, 1.0 mmol), compounds **3** (238 mg, 0.5 mmol), and 2-ethoxyethylamine (446 mg, 5.0 mmol) were dissolved in acetonitrile (8.0 mL), and the reaction mixture was refluxed for 12 h under argon atmosphere. The mixture was filtered, and the solvent was removed in a vacuum to give a yellow solid. The crude product was then chromatographed on silica gel using dichloromethane–methanol 15 : 1 (v/v) as eluant to afford 221 mg (84%) **M3** as a yellow viscous solid. ^{1}H NMR ($CDCl_3$, 400 MHz) δ 8.54 (d, J = 7.1 Hz, 1H), 8.47 (d, J = 8.0 Hz, 1H), 8.37 (d, J = 8.4 Hz, 1H), 7.64 (t, J = 7.8 Hz, 1H), 7.34 (s, 1H), 7.28 (s, 1H), 7.25 (d, J = 0.7 Hz, 1H), 7.17 (d, J = 8.1 Hz, 1H), 4.19 – 4.09 (m, 2H), 3.83 (s, 2H), 3.63 (s, 2H), 3.56 (t, J = 5.2 Hz, 2H), 3.49 (q, J = 7.0 Hz, 2H), 3.27 (s, 4H), 2.82 (t, J = 5.2 Hz, 2H), 2.75 (s, 4H), 2.29 (s, 2H), 1.68 (t, J = 7.5 Hz, 2H), 1.42 (dd, J = 15.0, 7.5 Hz, 2H), 1.18 (t, J = 7.0 Hz, 3H), 0.95 (t, J = 7.3 Hz, 3H). ^{13}C NMR ($CDCl_3$, 100 MHz) δ: 164.49, 164.02, 155.99, 139.33, 138.02, 132.52, 131.01, 130.27, 129.84, 129.25, 128.49, 128.11, 127.41, 126.12, 125.55, 123.27, 116.65, 114.86, 69.33, 66.50, 62.98, 53.60, 53.16, 53.04, 48.62, 40.06, 30.26, 20.40, 15.19, 13.88. HR-EI-MS calcd for $C_{32}H_{40}N_4O_3$ (M^+): 528.3100, found: 528.3096.

3. The absorption and emissive properties of NPO on changing the pH

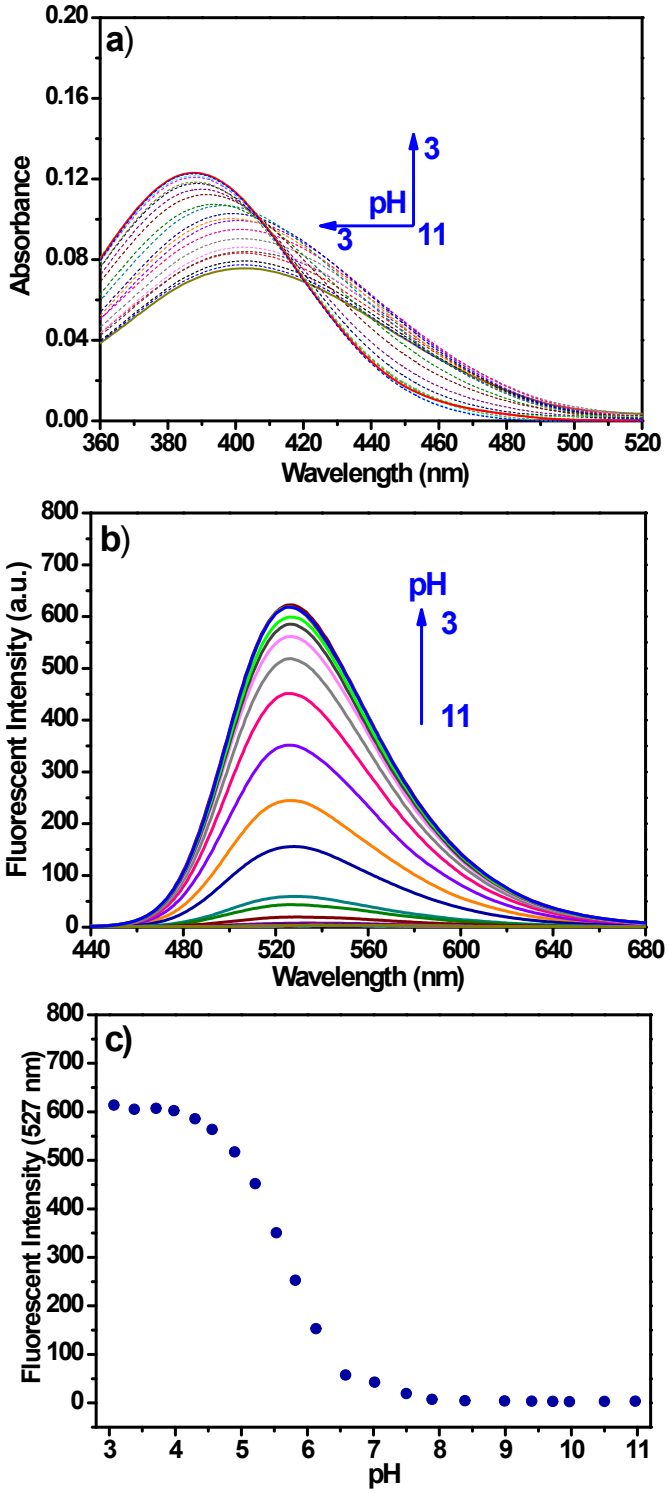

Fig. S1 The influence of pH on the absorption spectra (a) and fluorescence spectra (b) of **NPO** (10 μM) in water. (c) Curve of the maximum fluorescence intensity of **NPO** (10 μM) versus pH. (slits: 2.5, 5 nm.).

4. The absorption and emissive properties of NPC on changing the pH

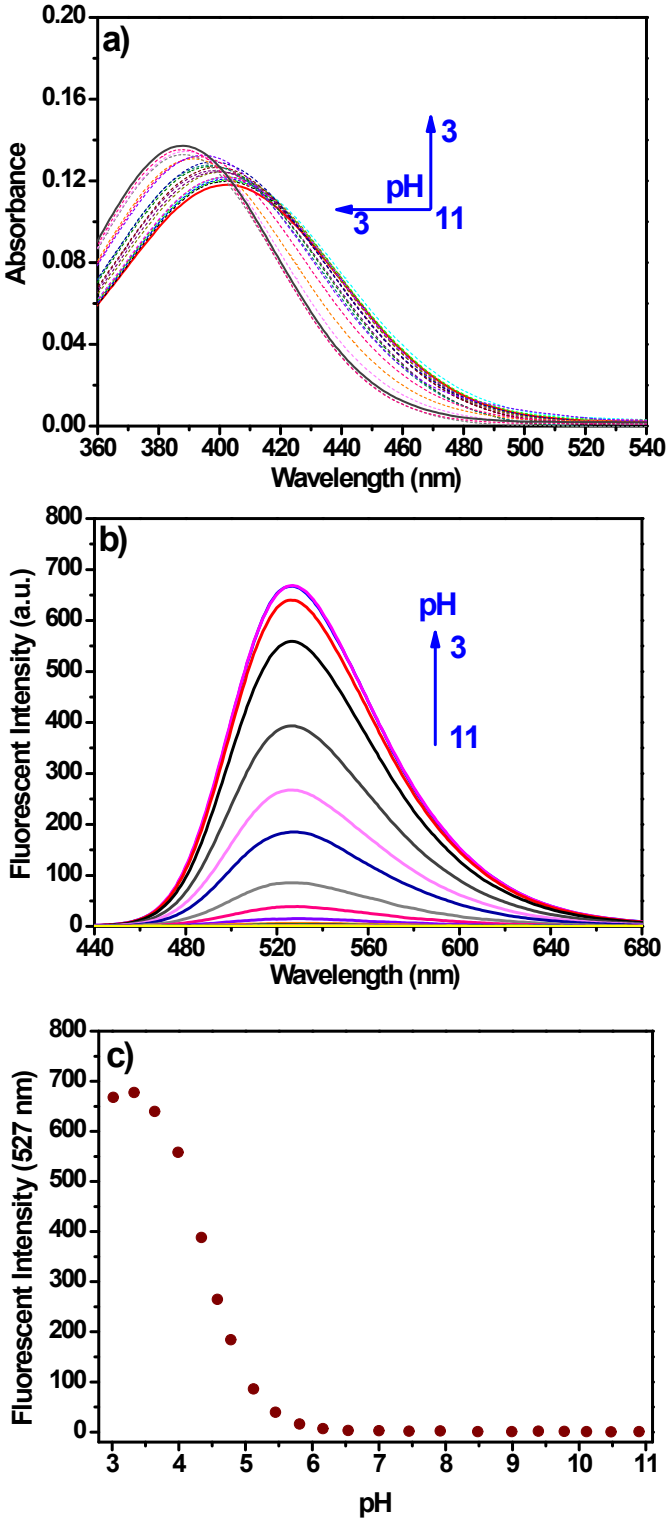

Fig. S2 The influence of pH on the absorption spectra (a) and fluorescence spectra (b) of **NPC** (10 μM) in water. (c) Curve of the maximum fluorescence intensity of **NPC** (10 μM) versus pH. (slits: 2.5, 5 nm.).

5. Fluorescence emission response of NPO in the presence of various metal ions

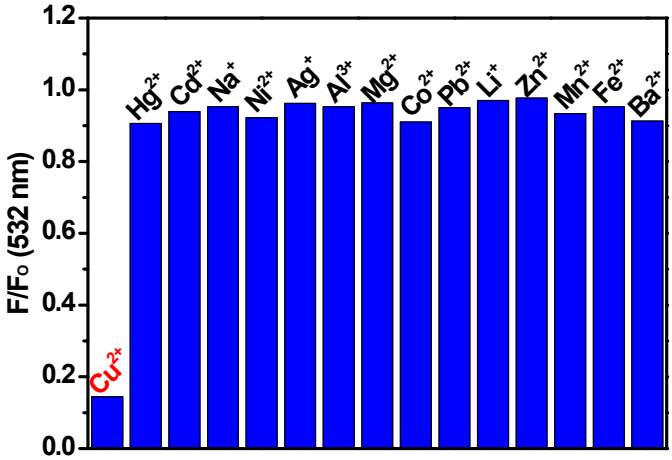

Fig. S3 Fluorescence emission response of **NPO** (10 μM) in the presence of various metal ions (all metal ions were 10 μM) in aqueous solution (10 mM HEPES, pH 7.4). (slits: 5, 5 nm).

6. Fluorescence titration of NPO with Cu^{2+}

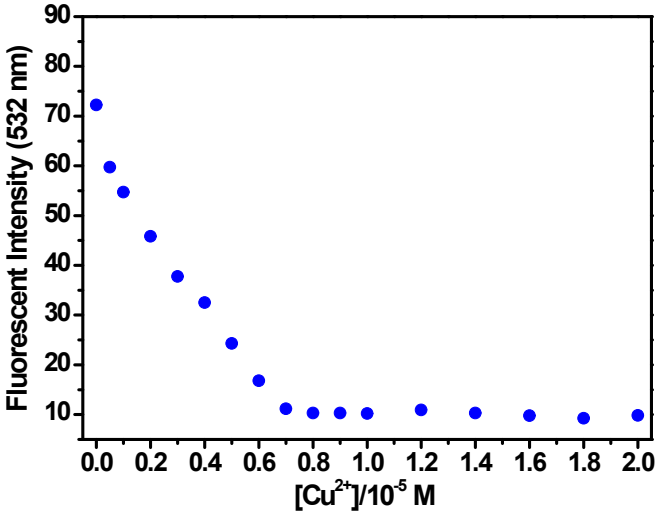

Fig. S4 Plot of fluorescence intensity at 532 nm of **NPO** versus concentration of Cu^{2+}. (slits: 5, 5 nm).

7. UV-Vis absorption titration spectra of NPO with Cu^{2+}

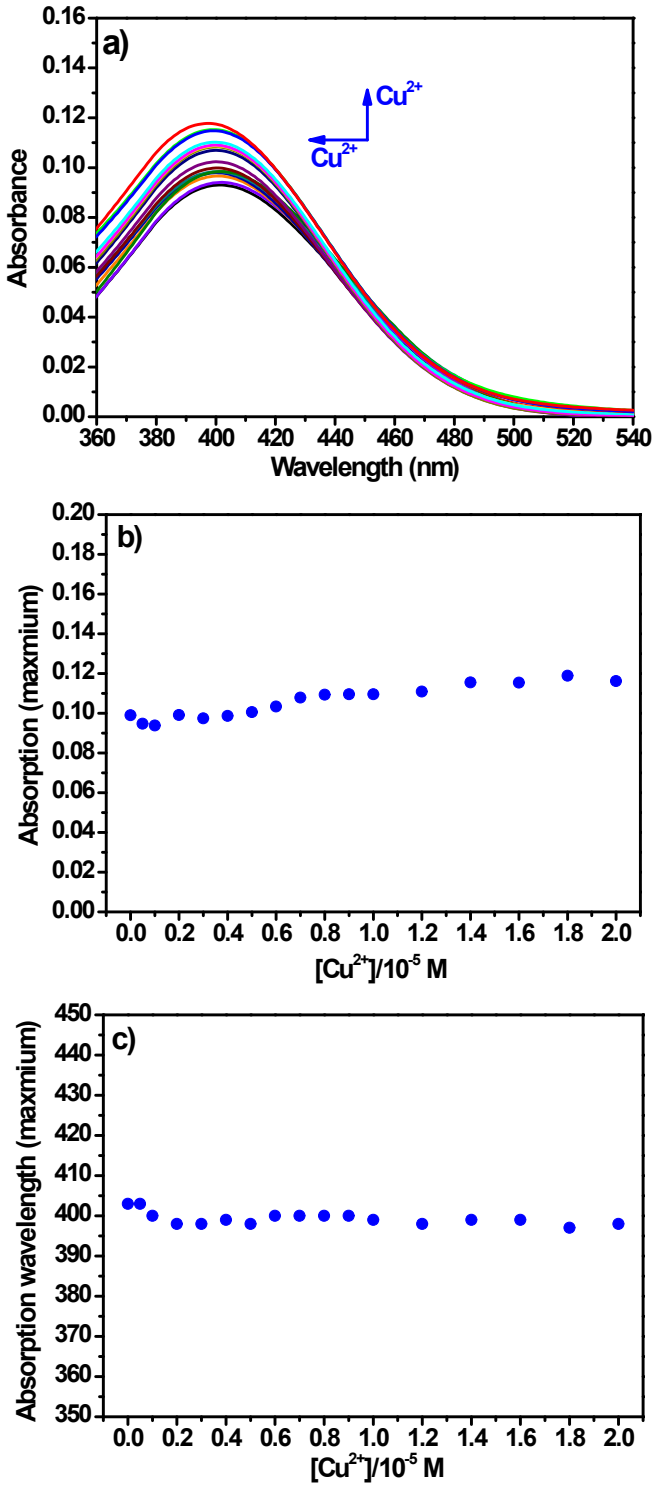

Fig. S5 (a) UV-Vis absorption spectra of **NPO** (10 μM) upon addition of Cu^{2+} (0.5–20 μM) in aqueous solution (10 mM HEPES, pH 7.4). The curves of maximum absorption (b) and the wavelength of maximum absorbance (c) of **NPO** (10 μM) versus increasing concentrations of Cu^{2+} (0.5–20 μM). (slits: 5, 5 nm).

8. Fluorescence and absorption spectra of NPC in the presence of various amino acids

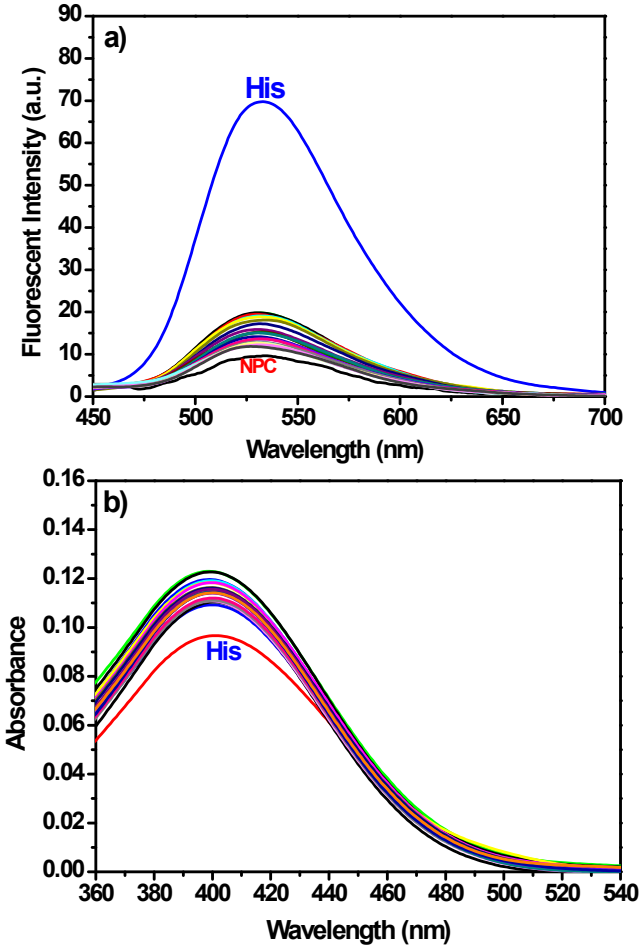

Fig. S6 Fluorescence (a) and absorption (b) spectra of **NPC** (the complex of 10 μM **NPO** and 10 μM Cu^{2+}) in the presence of various amino acids (all amino acids 40 μM) in aqueous solution (10 mM HEPES, pH 7.4).

9. UV-Vis absorption titration spectra of NPC with His

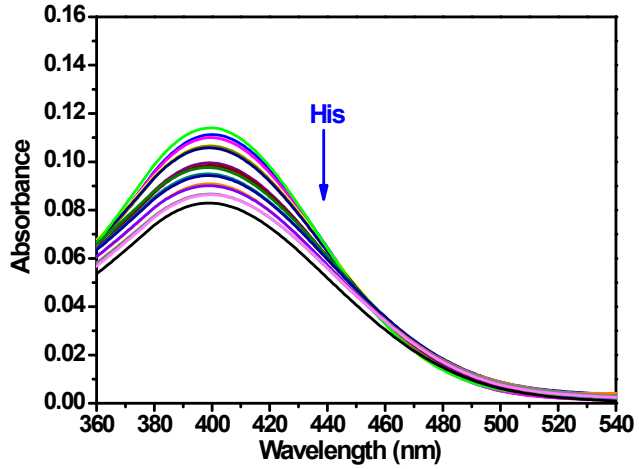

Fig. S7 (a) UV-Vis absorption spectra of **NPC** (10 μM) upon addition of His (2.0–51 μM) in aqueous solution (10 mM HEPES, pH 7.4).

10. The Job's plots of NPO with Cu^{2+} and NPC with His

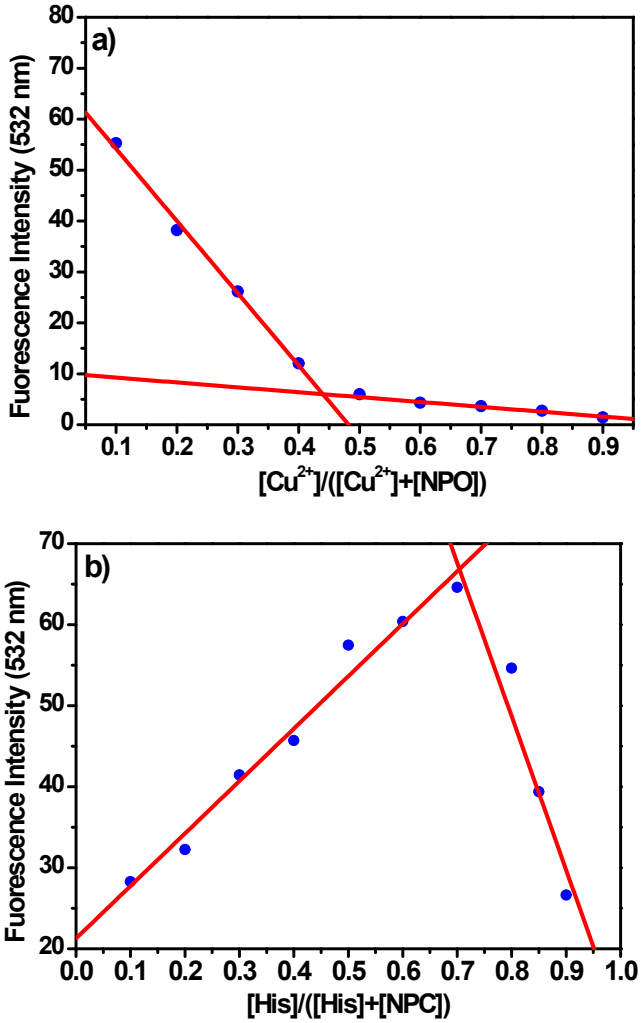

Fig. S8 (a) Job's plot of **NPO** and Cu^{2+} ([**NPO**] + [Cu^{2+}] = 10 μM) in aqueous solution (10 mM HEPES, pH 7.4). (b) Job's plot of **NPC** and His ([**NPC**] + [His] = 40 μM) in aqueous solution (10 mM HEPES, pH 7.4).

11. Fluorescence emission response of NPA-Cu^{2+} and M1-Cu^{2+} in the presence of various metal ions

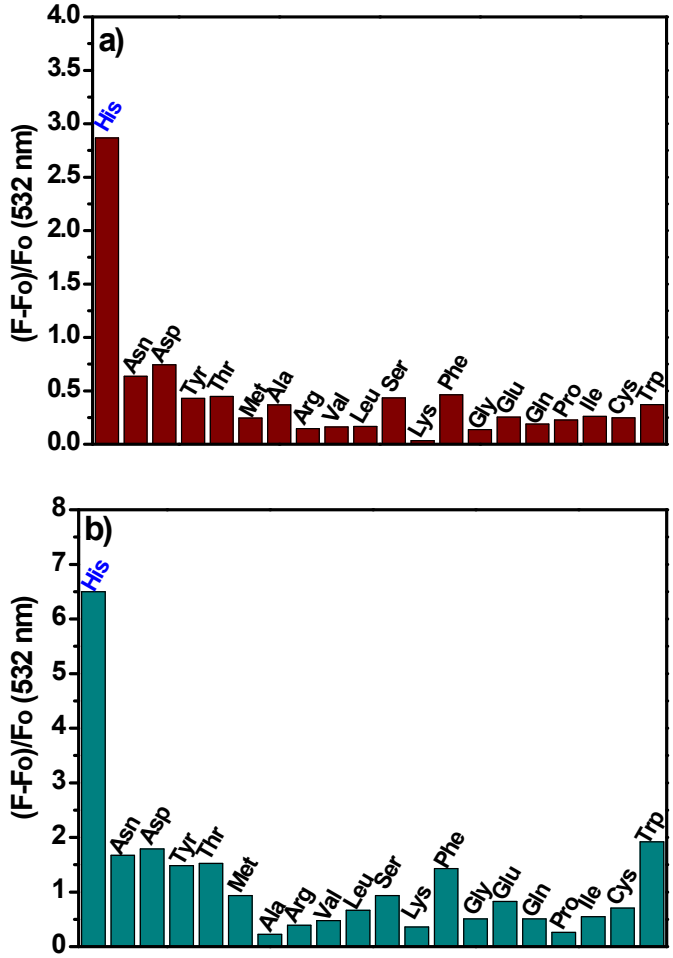

Fig. S9 Fluorescence intensity at 532 nm of (a) **NPA**-Cu^{2+} (the complex of 10 μM **NPA** and 10 μM Cu^{2+}) and (b) **M1**-Cu^{2+} (the complex of 10 μM **M1** and 10 μM Cu^{2+}) in the presence of various amino acids (all amino acids 40 μM) in aqueous solution (10 mM HEPES, pH 7.4).

12. The cytotoxicity of probe NPO against HeLa cells

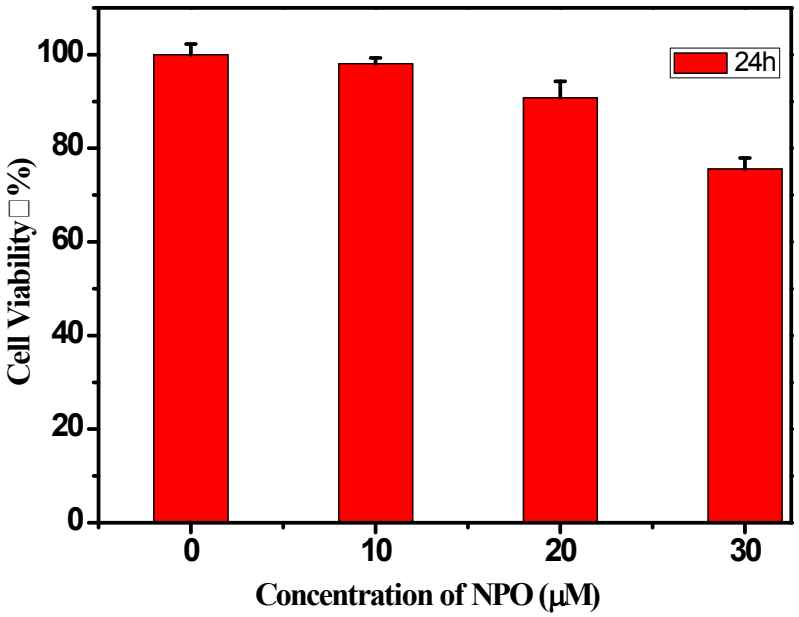

Fig. S10 Cell viability values (%) estimated by MTT test versus incubation concentrations of **NPO**. Cells were incubated with 10–30 μM **NPO** for 24 hours.